Cortical network mechanisms of anodal and cathodal transcranial direct current stimulation in awake primates

Andrew R. Bogaard[1,2,3,*], Guillaume Lajoie[4], Hayley Boyd[2], Andrew Morse[2], Stavros Zanos[5], Eberhard E. Fetz[1,2]

1) Department of Physiology and Biophysics, University of Washington, Seattle, WA, U.S.A. 2) Center for Neurotechnology, University of Washington, Seattle, WA, U.S.A. 3) Medical Scientist Training Program, University of Washington, Seattle, WA, U.S.A. 4) Département de Mathématiques et Statistiques, Université de Montréal, Montréal, QC, Canada 5) Feinstein Institute for Medical Research, Manhasset, NY, USA

Running Title: Cortical mechanisms of anodal and cathodal transcranial DC stimulation

Corresponding Author: Andrew R Bogaard

Email: abogaard@uw.edu

Number of text pages: 18

Number of figures: 7

Number of supplemental figures: 9

Acknowledgements: We thank Steve I. Perlmutter, Brian J. Mogen, and Marco Capogrosso for their invaluable consultations during the preparation of the manuscript, Rebekah Schaefer for animal care, and Larry Shupe for technical assistance. This work was supported by EEC-1028725 (ARB), F30NS100253 (ARB), R01NS12542 (EEF) and the NSF ERC Center for Neurotechnology

Abstract (191 words)

Transcranial direct current stimulation (tDCS) is a non-invasive neuromodulation technique that is widely used in clinical research to modulate cortical excitability and plasticity. At the same time, the mechanism of action and its actual impact on neuronal firing is unknown. To characterize potential effects of tDCS on sensorimotor neurons of behaviorally active cortical circuits, we implanted 96-channel microelectrode arrays in the sensorimotor cortex of two monkeys trained to perform a simple visuo-motor task. We recorded cortical spiking before, during, and after the most common forms of tDCS used in humans (unilateral sensorimotor stimulation) and found that neural responses were sensitive to both dose and polarity, and outlasted stimulation. Roughly 15% of cells were modulated by tDCS, and the ratio of excited to inhibited neurons was different for anodal and cathodal currents. At high currents, the cell-type specificity of these effects was indicative of direct effects on the neurons. Dynamics of neural ensembles during forearm contractions reflected dose-dependent changes in ensemble size and activation patterns. We conclude that tDCS induces reproducible and noticeable changes in cortical neuron activity at high doses, likely through a combination of single neuron polarization and network interactions.

Introduction

For nearly two decades, transcranial direct current stimulation (tDCS) has intrigued clinical and behavioral neuroscientists because there is evidence that it can produce clinical and behavioral gains. In its simplest implementation, tDCS is delivered through two sponge electrodes on the scalp to pass constant current across the head. Electrodes are placed in various montages with either a cathodal (c-) or anodal (a-) current delivered to the electrode over the target brain area, and the most common montage targets sensorimotor cortex (with the other electrode over the supraorbital area on the opposite side). In comparison to other techniques for stimulating the nervous system, tDCS stands out because applied currents are not strong enough to directly induce firing in neurons.

Human tDCS is derived from direct current, or polarizing, stimulation delivered to motor cortex in anesthetized rodents[1–5]. This form of weak stimulation modulated activity in a polarity-dependent manner: anodal stimulation tended to increase neuronal spike rates and the amplitude of cortico-cortical evoked potentials, while cathodal currents had the opposite effects. Particularly noteworthy was that these effects persisted hours if stimulation was delivered for at least about 10 minutes[2], an effect determined to require NMDA-dependent plasticity[3,6]. Recently, tDCS has been implicated in modulation of neurotransmitters at other synapse types and other mechanisms of plasticity, including GABAergic terminals[7,8] and BDNF release at glutamatergic synapses to promote plasticity in motor cortex[9].

tDCS is different from animal direct cortical polarization in significant ways that offer clinical advantages (non-invasive, safe, and cheap) at the expense of spatial selectivity and with a lower effective stimulation intensity (currents applied at the scalp are attenuated by shunting through soft tissue[10,11]). Despite the differences in application, aftereffects of stimulation are reported in human experiments as well. Perhaps the most influential example was an increase in the TMS-evoked MEP following anodal (a-) tDCS over motor cortex, and a corresponding decrease following cathodal (c-) tDCS[12,13], which resembled results from polarization experiments in animals. These seminal reports precipitated many studies that applied

tDCS in the hope of improving various neurological[14–16] and psychiatric conditions[17], and for use in behavioral neuroscience studies[18,19].

The number of tDCS studies grew dramatically over the past two decades, with experimental applications ranging from clinical rehabilitation (e.g. stroke[14] and depression[17]) to basic electrophysiology (e.g. TMS-MEP[13] and tDCS-EEG) and other physiological measures (e.g. magnetic resonance spectroscopy[7]), and behavior (e.g. reaction time and force production[20]). Overall, it appears that tDCS may be useful, but it still is not clear how to best use it, nor has it become easier to predict its effect for untested conditions[14,21–23]. For example, while a-tDCS was once thought to be excitatory and c-tDCS inhibitory, this relationship appears to depend on duration and intensity[24,25], brain state[26], and other factors. Physiological and behavioral results are also variable across studies, but these differences are hard to interpret because there is no standard methodology driving experiments across studies. Since the neural response to electrical stimulation is non-linear, small differences in delivery may account for such variability, but other factors such as anatomical differences between subjects with regards to brain, head shape, and extracranial tissue and hair[24,27] probably matter as well.

Considering the subthreshold nature of tDCS, a mechanism of action is hard to intuit and characterization of basic electrophysiological effects is challenging. Despite this, the field has made great strides towards uncovering the cellular and molecular changes associated with polarization, and has measured the intracranial manifestation of currents applied to the scalp. Now, multiple experiments have estimated the electric fields in the brain during scalp stimulation in monkeys[28,29] and humans[10,29,30], and showed that in humans they are at most about 0.5V/m. Although this data does not describe the brain response, *in-vitro* experiments suggest that fields of this magnitude can produce small (<1 mV) changes in the resting potential of the most polarized neuronal compartments[31,32], and neuronal networks in slice are sensitive to even weaker stimulation[33]. Neuronal polarization depends on morphology, orientation, and position of the soma[32,34], and can also selectively boost synaptic transmission and plasticity[35]. There is also reason to

believe that tDCS may be more specific than one may naively expect because active synapses, but not inactive ones, are potentiated during tDCS[9,35,36].

The consequence of such modest modulation of individual neurons on brain activity is not well known and remains a critical missing piece of data. The most common theory, sometimes called "amplification", proposes that these subthreshold effects bias the timing or gating of a neuron's spiking - a small effect occurring simultaneously in many neurons which propagates through the network and changes spatiotemporal dynamics at the network level. Models of neuronal networks suggest that subthreshold modulation can affect spike timing[37] and network dynamics[38]. At the same time, some cast doubt on the idea that such weak intracortical stimulation produces meaningful effects, suggesting instead that tDCS activates peripheral afferents of the cranial nerves innervating the scalp[10,39].

We aimed to characterize the effects tDCS on active sensorimotor cortical networks while monkeys alternated between coordinated movements and quiet sitting. Importantly, we applied both anodal and cathodal stimulation across a range of clinically-feasible current intensities over many days, often to overlapping populations of cells, which allowed us to systematically measure the differential effects across conditions. Since we recorded from single neurons, we wanted to compare responses (or lack thereof) of putative pyramidal and non-pyramidal cells to the patterns of modulation observed in vitro. We hypothesized that if tDCS acts primarily through polarization of brain cells and network "amplification", responses of neurons susceptible to polarization (e.g. pyramidal cells) would be sensitive to stimulation intensity and polarity. Additionally, we considered that responses of neurons less susceptible to polarization may reflect second-order, network-mediated effects driven by the population of polarized cells.

At the same time, firing rate responses might not be appropriate for detecting tDCS induced changes, because such weak subthreshold modulation may only affect the timing of action-potentials[37]. In this case, effects of tDCS should be evident in ensemble dynamics. Therefore, we used a two-pronged approach: first, we analyzed the patterns of firing rate changes in cells and used spike waveform analysis to label

putative pyramidal and non-pyramidal cell types. Secondly, we determined whether the ensemble firing patterns in neural populations are altered by tDCS.

Results

Changes in single-unit firing rates during tDCS

The sensorimotor cortex is a common target for tDCS, particularly in trials to treat stroke[40,41]: the most common montage places one pad over sensorimotor cortex, and the other over the contralateral supraorbital area[13,42,43] (**Fig. 1a**). Human tDCS electrodes are roughly 5x7cm in size, and current densities are low (0.028mA/cm^2 to ~0.1mA/cm^2)[44]. Similar to these human trials, we delivered tDCS through saline-soaked cellulose sponge electrodes (**Fig. 1b**) and applied current densities that ranged from low in human studies (0.027 mA/cm^2, 0.25mA) to about four times that currently used in humans (0.44 mA/cm^2; 4mA). We designed the experiment to characterize the patterns of activity of cortical firing during different doses and polarity configurations of clinical-type tDCS, but do not claim to replicate the precise stimulation conditions that are present in humans. This is because such values are likely to vary from person to person, and also because the same current applied to monkeys will produce different intracranial fields due to differences in skull thickness, soft tissue composition, and differences in brain structure of monkeys and humans (*Supplement: Limitations*).

Monkeys performed a visuomotor target-tracking task by controlling the position of a cursor via isometric wrist torques registered by a 2-axis manipulandum (**Fig. 3a**). The task was intentionally designed to be simple and over-trained in order to maintain tight behavioral control and to isolate simple physiological changes in neuronal activity related to motor performance, but avoid confounding effects introduced by high-level cognitive processes (e.g. attention, learning). During each trial, the monkey was cued to move the cursor to one of eight targets by contracting his forearm muscles to produce isometric torques in wrist flexion/extension and radial/ulnar dimensions, and the task ran for the duration of the experiment. As anticipated, tDCS had little to no effect on the monkey's ability to perform the task (**Supplementary Fig. 1**), thus eliminating any potential confounds from behavioral changes induced by tDCS.

Single unit activity (SUA) was recorded from the gyral crown by 96-channel microelectrode arrays (**Fig. 1c**) before, during, and after tDCS (**Fig. 1d**, Pre, Stim/Sham, and Post epochs, respectively), and we followed strict cell inclusion criteria similar to other studies (Supplement: Cell inclusion criteria). Over the course of 109 experiments (45 Sham, 29 a-tDCS, 35 c-tDCS) we obtained 2671 isolated unit recordings. The waveform and firing statistics of some of these units suggested that we recorded from the same neuron across days, so we used a cell identification algorithm similar to those previously reported to identify them (*Supplement: Longitudinal cell analysis*). Out of a total of 2671 neurons, the algorithm detected 1178 unique cells.

Units isolated before the onset of tDCS were reliably recorded during stimulation, as shown in the single-unit band of the recorded local field potential (**Fig. 1d**). We tracked relative changes in firing rates during the experiments for each neuron, ΔF_t^i, as $100 \cdot (F_t^i - F^i_{PRE}) / max(F^i_{PRE}, F_t^i)$ where F_t is the firing rate for neuron i at time t and F^i_{PRE} is the mean firing rate during the "Pre" epoch. **Figure 1e** shows ΔF for all neurons during successive minutes throughout anodal tDCS. We found that both high dose (>1mA) and low dose (≤1 mA) a-tDCS increased firing rates within the first minutes of stimulation. At high doses, increased firing persisted for about 15 minutes after tDCS was turned off ("*" **Fig. 1e**, Wilcoxon rank-sum test $p<0.01$).

We also analyzed whether ΔF was different for anodal versus cathodal tDCS. **Figure 2a** shows that there was a dose-dependent increase in population firing rate during a-tDCS (red data points, sigmoid dose-response curve, *Supplementary Eq.* 4, **Supplemental Fig. 2** shows results by experiment). Maximal sensitivity to tDCS intensity was similar for both monkeys (dose-response midpoint; S: 1.2mA; W: 1.14mA). Interestingly, c-tDCS produced no statistically significant increase or decrease in the population firing for any stimulation intensity (**Fig. 2a**, black data points). It should be stressed, however, that this analysis is not sensitive to effects with mixed firing rate changes (i.e. if some neurons were modulated up while others were modulated down), or effects in a small subset of neurons. Thus, we also performed a cell-by-cell analysis of changes in firing rate.

Percent of cells modulated by tDCS

Population-wide statistics depicted in **Figure 2a** may mask mixed effects in individual cells, so we examined whether tDCS impacted the likelihood that any individual cell's firing was increased or decreased. **Figures 2b and c** show the percent of neurons with a given change in firing across three conditions. During high dose a-tDCS, a higher percentage of neurons exhibited increased firing ($\Delta F > 0$), and a lower percentage showed decreased firing ($\Delta F < 0$) than during Sham or c-tDCS (**Fig. 2b**), in agreement with population averages. Interestingly, during high dose c-tDCS, a higher percentage of neurons had increased or decreased firing as compared with Sham, indicating that c-tDCS indeed affected firing, but the effects were mixed. To highlight this, **Figure 2c** shows the percent of cells with an absolute change in firing greater than or equal to a given $|\Delta F|$. More cells had larger absolute firing rate changes during both a- and c-tDCS, and the percent of cells affected by c-tDCS is comparable to that affected by a-tDCS. Differences from Sham were more pronounced for larger absolute changes in firing – for instance, neurons were about 1.5x more likely to be undergo a >20% change during a- and c-tDCS (corresponding to about 10-15% of neurons).

We also estimated the percent of neurons affected by tDCS by labeling cells as modulated up or down if their mean firing rate during high dose tDCS or Sham exceeded 3·SD from the baseline during Pre. Using these criterion, results were similar to data presented in Figure 2d-e. Neurons were more than twice as likely to change their firing during tDCS as compared with sham, a higher percentage were modulated up than down during a-tDCS, while c-tDCS increased the likelihood that cells were modulated either up or down. This mixed effect explains why average population firing rate changes were not obvious during c-tDCS (**Fig. 2a**).

Direction of modulation depends on cell type

Why might firing rate changes be mixed for a given polarity? Modeling and experiments in-vitro suggest that the effects of tDCS on single neurons will depend on their morphology[31] and orientation[32]: anatomical factors that correlate with cell type. Neurons with a major somato-dendritic axis in parallel

with the induced electric field (such as pyramidal cells) should be more susceptible to somatic modulation by tDCS, whereas those without a dominant axis or with a centrally positioned soma (such as interneurons), would not be as directly affected. Cell-type specific optogenetic stimulation has shown that the width of the extracellularly recorded action potential is well correlated with these two broad classes of neurons[45] (although it has limitations[46]) – narrow spike widths correspond with "fast spiking" (FS) putative interneurons and broad spike widths with "regular spiking" (RS) putative pyramidal neurons. As shown in **Figure 2d**, the distribution of spike waveform width is bimodal. The average spike shape of each cluster is indicated in green (RS cells: ≥250μs, N=1812) and blue (FS cells: <250μs, N=859). Consistent with other studies, FS firing rates were higher than that of RS firing rates, and exhibited task-related dynamics that were similar between monkeys (**Supplemental Fig. 3**)

tDCS affected both RS and FS cells, but the changes in RS cell firing rates during tDCS were greater and sensitive to polarity. On the other hand, responses of FS cells were not sensitive to polarity. **Figure 2e** shows the spiking responses to a- and c-tDCS at different doses for RS and FS neurons separately. Note that firing rates of RS cells tend to get faster with increasing anodal currents, and slower with increasing cathodal currents. FS neurons are less correlated with tDCS intensity, but tend to increase firing in both conditions. Shown this way, it is clear that population effects of c-tDCS are obscured by hetereogeneous responses related corresponding to cell type (**Fig 2a**). The finding that RS neurons are more sensitive to polarity than FS neurons is consistent with the "somatic" theory of tDCS, which predicts that the position of the soma along the morphological axis in parallel with the electric field is an important factor in the single-cell effect of tDCS. At the same time, it is intriguing that such effects are evident in neuronal networks during natural processing.

The same neurons are consistently modulated by tDCS

Given that such a relatively small fraction of cells were affected during tDCS, it was important to determine whether these changes were repeatable. Neurons were identified across experiments using a combination of previous methods[47–49] (*Supplement: Longitudinal analysis,* **Supplemental Fig. 4-6**) and

the algorithm classified 1178 potentially unique neurons, 518 of which were recorded more than once (**Supplemental Fig. 5**). **Figure 3b** shows a typical example neuron recorded across four cathodal experiments, one sham experiment, and two a-tDCS experiments. The firing rate of this neuron decreased proportionally with c-tDCS intensity, but the pattern of firing in torque space (firing rate heat maps and directional polar plots) was preserved. For this neuron, firing rates remained constant during Sham and low-dose a-tDCS experiments (there were no high dose a-tDCS experiments with this neuron).

Once cells were identified across experiments, we calculated the percentage of neurons consistently excited or inhibited during each condition (**Fig. 3c**, insert shows an example for down-regulated neurons during c-tDCS). We tested the null hypothesis that neurons exhibited consistent firing rate changes by chance alone using a shuffling algorithm (*Supplement: Shuffle distributions*), and found that both a- and c-tDCS had significant repeat excitatory and inhibitory effects (**Fig. 3c,d**, z score>5.3 or $p<0.001$). Interestingly, about 13% of neurons consistently modulated their firing during Sham (**Fig. 3d**, $p<0.05$), but neurons were about 2.5x more likely to undergo the same direction of firing rate changes during high dose a- and c-tDCS (**Fig. 3c,d**). This finding suggests that effects of tDCS are repeatable at the single cellular level. Furthermore, this analysis demonstrated that a-tDCS decreased firing in some neurons (**Fig. 3d**, *Always decrease*, z-score=5.3 or $p<0.001$), an effect that was not obvious from changes in firing rate changes alone.

Single neuron tuning

Changes in spiking threshold can alter neuronal tuning by either sharpening or broadening the rate function[50,51]. We investigated whether tDCS disrupted task-related firing by analyzing neuron tuning to torque direction and torque space maps, which were prominent in both monkeys. To analyze a neuron's preference for a given torque direction, we calculated the mean resultant vector (MRV) from the directional tuning function. The magnitude of the MRV (R_L, *Supplementary Eq.* 6) describes the degree to which a neuron is directionally tuned, and its direction (φ_R, *Supplementary Eq.* 7) indicates the preferred direction. Both measures are independent of firing rate and estimate the shape of tuning only, therefore,

firing rate changes induced by tDCS would not alone produce changes in R_L or φ_R. **Figure 4a** shows the peak-normalized torque direction tuning curves for all recorded neurons ordered by R_L and rotated so that φ_R align. About one third of neurons recorded in each monkey were directionally tuned (R_L>.1; Monkey S: 33.6%, Monkey W: 35.8%). In these neurons, tDCS did not induce changes in the direction or strength of tuning for any dose. In particular, **Figure 4c** depicts the change in tuning strength (R_L) for all tuned neurons from Pre to tDCS/Sham epochs and shows that there is an equally small drop (about 5%) in tuning strength in all conditions, indicating that even high dose tDCS had no effect in tuning strength as compared to Sham. Similarly, **Figure 4d** shows that the variability in directional tuning during tDCS was no greater than during Sham.

Beyond directional tuning, many neurons showed phasic task activation, such as increased firing during the hold phase, rest phase, early contraction, etc. (see example neuron in **Fig. 3**). These correlations are reflected in the torque space firing rate map as hot spots, and we used these rate maps to assess cell tuning similarity (Pearson's correlation coefficient, ρ) and specificity (information per spike, I[52]) across epochs. **Figure 5a and c** explain how ρ and I vary with changes in the rate map. We found that cell tuning was relatively stable during the experiment (**Fig. 5b,** Sham), and high dose tDCS produced a small but significant drop in ρ that reflected minor shifts in the rate map which exceeded those observed during Sham. Low dose tDCS did not produce this change (**Fig. 5b**). Rate map shifts did not correspond with decreases in firing specificity (I) during tDCS experiments although they did during Sham (**Fig. 5d**). From these analyses we note that tDCS had very minor to no effect on single neuron tuning. At the same time, such single unit analyses may not be an adequate or appropriate measure for detecting the collective action of tDCS on cortical networks (e.g. alterations in the timing and joint firing of neural ensembles in the network may not result in rate changes).

Neural population dynamics

The collective action of tDCS on active cortical networks may be most sensitively detected in population activity, which comprehensively describes neural activity associated with movement[53–56]. To test this, we

quantified activity of the recorded ensemble in a "neural space" whose dimensions corresponds to the firing of individual neurons[56–58]. We used a version of demixed principal component analysis (dPCA)[59,60] to extract the most informative linear subspaces (manifolds) within ensemble trajectories during the task, and asked: (1) does tDCS affect the size of functional neural ensembles? and (2) does tDCS change the spatiotemporal activation patterns of ensembles?

Similar to previous studies[57], we analyzed smoothed spike trains (Gaussian filter σ=100ms) from 0 to 500ms after target appearance (this period contained neural activity most relevant to stereotyped contractions during the task). On each trial, the spike trains of every neuron were normalized to zero mean and unit variance (over the time course of that trial) to mitigate the biasing effects of heterogeneous firing rates across neurons and tDCS-induced firing rate changes (though results were similar without normalizing for mean firing rate). Normalized spike trains were averaged across trials conditioned on target number (demixing step), and then standard PCA was performed on the concatenated, target-specific, N_{cells}-dimensional spike rate functions (for experiments where $N_{cells} \geq 10$) for each experiment epoch (*Supplement: population analysis*). As evident in **Figure 6a**, averaged ensemble trajectories projected into epoch-specific 2-D manifolds were well separated for the different targets, and even resembled torque trajectories, indicating that neural population dynamics in the space of the first two principal components reflected motor activity.

We used two measures to test whether the dynamic organization of the ensemble shifted during tDCS (*Supplement*: *Neural population dynamics*). First, we calculated the *dimensionality* (*D*) of the ensemble trajectories[61,62]. If all neuronal firing is highly correlated, points in the neural space approach a line ($D=1$), whereas if all neurons are firing independently, points are dispersed throughout the neural space ($D=N_{cells}$). Population activity is typically restricted to a smaller subspace ($1<D<<N_{cells}$), which is thought to reflect functional connectivity of the network[56]. In our experiments, *D* was similar across experiments (5.20±0.15). Interestingly, we found that the dimensionality of ensemble trajectories decreased with time under normal conditions (Sham, **Fig. 6b**), whereas a- and c-tDCS both increased *D*

(**Fig. 6b,** independent t-test Sham vs tDCS; a-tDCS p=0.002, c-tDCS p=0.012). Qualitatively, this result indicates that tDCS disturbed engrained ensemble dynamics and increased the working neural space during contractions. This effect was only significant for high doses, and was most pronounced during a-tDCS. Increases in ensemble dimensionality persisted after tDCS was turned off (**Supplementary Fig. 9**).

We also tested whether new dominant patterns of activity arose during tDCS by measuring the principal angles between the intrinsic manifolds (PC1 & PC2) as schematized in **Figure 6c$_i$**. This angle of similarity, S_{ori}, was calculated as the mean cosine of principal angles and ranges from 0 (orthogonal ensemble activity) to 1 (unchanged). Manifold orientation changed very little during Sham epochs (S_{ori} = 0.87; **Fig. 6c$_{ii}$**), indicating that ensemble activity patterns were stable over time. c-tDCS and low dose a-tDCS did not produce shifts in the manifold, but there was a significant shift during high dose a-tDCS (**Fig. 6c$_{ii}$**; a-tDCS thick bars, p=0.02), and this result weakly persisted after a-tDCS was turned off (**Supplementary Fig. 9,** p=0.059). Thus, high dose tDCS produced ensemble activity outside of the existing subspace, and a-tDCS was more effective at eliciting new dominant ensemble patterns than c-tDCS.

Features in spike-triggered LFP are diminished during tDCS

Finally, we investigated the effects of tDCS on synaptic currents correlated with neuron spiking observed in the LFP using the whitened spike-triggered LFP (wst-LFP)[63]. This method calculates the average spike-triggered LFP at multiple electrode sites and applies a spatial filter to separate the effects of a single neuron from non-specific components of the LFP which are common across the whole array (e.g., beta oscillations). Consistent with previous studies[63], wst-LFP from our arrays support the notion that resultant features are synaptic currents evoked by spikes of the triggering neuron: they occurred after the spikes (**Fig. 7a,b**), and were restricted to electrode sites close to the neuron within known limits of axonal projection[64] (**Fig. 7b,c**).

wst-LFP features are consistent throughout recordings without stimulation (**Fig. 7c**). During high dose a- and c-tDCS, however, there was a significant decrease in wst-LFP features for adjacent channels (0.4 and

0.8mm) when all cells were considered. Upon further inspection, we found that fields from RS cells were more affected by a-tDCS, while those from FS cells were more affected by c-tDCS. **Figures 7d,e** show how high dose tDCS affected RS (**d**, green spike) and FS (**e**, blue spike) neurons. Notably, changes were restricted to neighboring electrode sites. Low dose tDCS did not produce any significant changes (≤1mA, $p>0.05$). See *Supplemental Table 1* for fit parameters and corresponding N for Figures 7d,e.

Discussion

These experiments documented dose-dependent responses to tDCS in primate sensorimotor cortex by tracking single cell firing rates, and also by analyzing ensemble dynamics. During the experiments, monkeys actively participated in a simple target-tracking task requiring isometric contractions about the wrist. Since we aimed to test for potential effects mediated by direct cellular polarization, we designed the task to be simple and over-trained to control against behavioral differences related to learning (e.g. performance gains/losses). Monkeys performed the task continuously and without significant changes in performance.

Implications for human tDCS

While our findings cannot be mapped directly onto humans with regards to current intensity, studies with non-human primates provide a unique opportunity to observe intracortical effects under circumstances similar to those used in humans. Finite element models of monkeys with a similar preparation (Utah array, two-electrode tDCS each with area 3.14cm^2) suggest that at 2mA the intracranial fields in macaca mulatta will be about 0.2-0.7 V/m[65], and recordings at multiple depths in two monkeys found that 1mA tDCS resulted in median field of 0.2 and 0.4V/m respectively[29]. For reference, electric fields in humans during tDCS have now been measured at between 0.05-0.5V/m[10,29,30] for 1mA tDCS. To measure the fields in these studies, electrodes were placed along the gradient expected between the stimulating electrodes. Electrodes of the Utah array, on the other hand, are orientated tangentially to the cortical surface, which maximizes the number of neurons recorded, but are limited for estimating the currents

induced in the brain by tDCS. Moreover the electrode tip capacitance does not allow accurate measures of DC potentials. Thus, we have not reported estimations of the electric field (as similar to another study[65]).

There was a notable difference in firing rate responses between the two monkeys used in our study, which may be due to inter-subject differences. A previous study measured intracranial fields using multi-depth EEG depth electrodes in two anesthetized monkeys: one female, and another, larger male with more epicranial muscle. The authors found a nearly twofold difference in electric field magnitude between the two monkeys, with more current reaching the brain in the smaller one[29]. In our study there was a sizable difference in weight and head shape between the monkeys as well: monkey S was significantly larger and had more extracranial muscle mass than monkey W (14kg versus 10kg). In agreement with this past study, the effect size in the larger monkey was smaller than that observed in the smaller one (**Figure 1a**), suggesting that these anatomical differences played a role. Another significant difference is that the array was placed in precentral cortex in monkey S and postcentral cortex in monkey W.

Even though the exact stimulation amplitudes cannot be compared to human tDCS, our results confirm that tDCS current intensity is a critical parameter – larger currents produced larger effects in disparate measures such as single cell firing rates, rate-normalized population dynamics, and the wst-LFP. We found effects in the primate brain at current densities within clinical safety limits, but at levels that were higher than those generally used in humans ($0.11 mA \cdot cm^{-2}$). The highest current densities applied to the skin in our study are about four times greater than those currently used, although comparable protocols have been used before. Between 1960 and 1998, a few studies[66] delivered tDCS through much smaller scalp electrodes with current densities of $0.2 mA/cm^2$, well within the range of effects in our study. One older study successfully applied 2.4 mA/cm^2 to one patient with local anesthetic under the electrode[67].

Effects in firing rate

Neurons are susceptible to externally generated electric fields to varying degrees, and the pattern of hyperpolarization and depolarization in single neurons depends upon its morphology and orientation in the field[31–33,38]. Likewise, synaptic transmission is also affected, and can be boosted or inhibited both pre-

and post-synaptically[35,36], as noted from slice preparations of the rodent hippocampus, a structure with very regular ordering of the principle neurons and their inputs. From this it is difficult to infer the cumulative effects of such distributed polarization across the cortex, with its full connectivity and intrinsic dynamics during behavior. For instance, although principle cells may be more susceptible to direct polarization by tDCS, extrinsic excitation or inhibition of these cells could propagate through intermediate inhibitory cells to produce unpredictable network-level effects. Thus, characterizing the responses of neurons in active cortical circuits was one of the main goals of our study.

We detected firing rate changes in about 15% of neurons during a- and c-tDCS as compared with Sham tDCS. Although the percent of cells modulated during a- and c-tDCS was similar, the proportion of neurons with increased firing was much higher during a-tDCS (9:1) than c-tDCS (3:2). Importantly, the same percentage of cells, 15%, was found when estimating the percent of neurons that reliably modulated their firing in the same direction for repeat a- or c-tDCS. Overall, despite differences day-to-day in the composition of neurons sampled, the average response to a given polarity and dose was surprisingly repeatable across days for individual neurons (**Supplemental Fig. 2**); not only were the average population statistics similar across days, single neurons were also more likely to be consistently modulated up or down by high dose tDCS.

The fact that firing rate changes were only detectable in a subset of neurons is not necessarily surprising. Neurons differ in their response to polarizing currents, and even in the most polarizable neurons, various cellular compartments may undergo a very modest (<1mV) change in membrane potential, depending on the pattern of depolarization and hyperpolarization induced by the electric field. While some network models have predicted that such changes could produce changes in spiking timing[37,50], it was not clear whether tDCS would produce changes in firing rates. In fact, an earlier study did not detect firing rate changes[65], a difference that may be due to the smaller sampling of neurons, or because only one lower intensity current was applied for short time intervals.

We checked whether firing rate changes matched the weak modulation of individual neuron types demonstrated in-vitro. Our recordings came from a depth of 1.5 mm at the gyral crown, directly under the stimulating electrode where the electric fields are strongest[10] and are expected to be radial to the cortical surface. Direct polarization by tDCS should be most pronounced among cortical pyramidal neurons[31], putatively identified here using cell waveform analysis. Though imperfect[46], this classification yielded two population of neurons that were differently affected by polarization. Firing rates of putative pyramidal neurons changed in accordance with tDCS intensity and polarity – increasing with anodal stimulation and decreasing with cathodal stimulation. In contrast, the firing rates of putative inhibitory cells positively correlated with tDCS intensity regardless of polarity, which may be the result of dendritic depolarization, or secondary to network effects following the primary modulation of other cell types. Errors induced by this method of cell identification would lead to an underestimation of cell-type dependency on polarity, so this effect may be larger than we could detect.

It is conceivable that such changes in firing rate would affect neuron tuning curves. For example, if neuronal tuning is similar to an "iceberg"[50,51], one might expect tuning to become more dispersed when the soma is depolarized, and sharper when it is hyperpolarized, due to a relative shift in spiking threshold. However, we did not observe obvious changes in the broadness or direction of single unit tuning, suggesting that tDCS did not simply increase excitability at the expense of selectivity. Effects were similar in both pre- and post-central gyrus, which have analogous structures and overlapping functions[68–70]. In both cases, tuning to torque was preserved, which presumably reflect a mixture of both efferent and afferent cortical signals. It therefore seems likely that responses in other cortical areas with analogous cell organization will be similar.

Network level effects and ensemble dynamics

Although we observed lasting firing rate changes in a fraction of recorded neurons, this is not a very sensitive measure. Instead, when recording neural ensembles, metrics that quantify activity at the population level are more appropriate and nuanced. Ensemble dynamics are confined to a small part of

the total neural space[56] (the manifold); and activity unexpressed by the population (areas outside of the manifold) are probably determined by functional connectivity patterns in the network[56]. New patterns of activation produce subsequent shifts in the manifold once learned, and tasks associated with points farther from the manifold (neural associations rarely expressed) take longer to learn[56,71]. In our experiments, dimensionality of ensemble trajectories increased during tDCS, although it tended to *decrease* with time otherwise. This finding is consistent with theories underlying the warm-up effect, in which a network refines its activity during practice of a rehearsed task[72]. Conversely, increasing the dimensionality (and therefore dispersion) of firing during tDCS may explain tDCS-associated increases in learning rates: by increasing the size of the working neural subspace, new, successful patterns can be more quickly tried and reinforced[73]. Therefore, it appears that high dose tDCS releases constraints imposed by functional connectivity patterns (by dendritic depolarization, disinhibition, etc.) to augment learning from otherwise deeply embedded associations.

Spike-triggered fields

Features of the unitary LFP (postsynaptic currents initiated by spiking, wst-LFP[63]) were diminished by tDCS in a dose-dependent matter, suggesting that tDCS influences synaptic transmission. Deflections in the wst-LFP are thought to reflect inhibitory postsynaptic potentials in apical dendrites of pyramidal cells[63]. tDCS decreased the amplitude of these currents, an effect most pronounced among RS cells during a-tDCS, which coincided with a global increase in firing. These findings are consistent with direct modulation of RS cells by tDCS with a consequent drop in feedback inhibition and decreased inhibitory drive while the apical dendrites are predicted to be hyperpolarized. Also, the larger decrease in wst-LFP associated with RS, but not FS, cells could be due to divergent effects resulting from documented connectivity patterns from RS neuron to many inhibitory interneurons[74]. Decreases in RS firing during c-tDCS did not correspond with an increase in wst-LFP, suggesting that c-tDCS directly inhibited RS cells. One puzzling result is the decrease in wst-LFP associated with FS cells during c-tDCS, a condition when

the apical dendrites of pyramidal cells are predicted to be relatively depolarized. Future studies in vitro may elaborate on this interplay between simultaneously polarized synapses and neurons.

Peripheral effects

Besides the theory of direct neuronal polarization and network amplification, some have proposed that effects of transcranial stimulation are mediated by afferents of the cranial nerves innervating the scalp[10,39]. Furthermore, acoustic or visual disturbances reported to coincide with high intensity tDCS could also produce changes in brain activity, and must be taken into account when interpreting these data. We do not believe that the changes in spikes we observed are due to such peripheral effects for several reasons. First, the monkeys did not appear to notice the stimulation, and continued to perform the task at rates/torques nearly identical to pre-stimulation epochs (**Supplemental Fig. 1**). Monkeys are very sensitive to such changes, and skin, acoustic or visual distractions would have likely resulted in marked behavioral changes. Second, recordings from both monkeys were collected from an area of cortex innervating/innervated by the contralateral forelimb, so it is unlikely that observed changed were due to activation of the trigeminal nerve.

We cannot rule out that tDCS stimulated afferents from the scalp, but we would not expect such activation to produce the changes we observed in sensorimotor cortex in the absence of gross behavioral changes. Tingling or burning sensations would be similar for anodal and cathodal stimulation, and in this hypothetical case, alterations brain activity would not be different for the two conditions. However, there was a very significant difference in the responses evoked by anodal and cathodal stimulation. First, the proportion of neurons excited/inhibited varied, and second, the pattern of excitation/inhibition in single neurons matched the expected patterns given by their cell type.

Conclusions

The clinical utility of tDCS depends on additional physiological data that will refine the protocol and test the theories underlying its mechanism of action. Most believe that intracranial current from tDCS directly

polarizes neurons in the brain, but this has been called into question. To address this, we examined the patterns of modulation across populations of cortical neurons and found effects consistent with direct neuronal modulation during anodal and cathodal tDCS at high current intensities. Quantification of ensemble dynamics demonstrated that anodal tDCS was more effective at shifting network activation patterns, but both polarities expanded the active neural space and had effects that outlasted stimulation. Thus, at sufficient doses, it appears that tDCS acts on underlying cortex through a combination of cell polarization and second-order network mediated interactions. Future studies could investigate the potential for these changes to beneficially affect learning and plasticity in the behaving primate, and to further bridge the gap between animal models and human tDCS.

Figure Legends

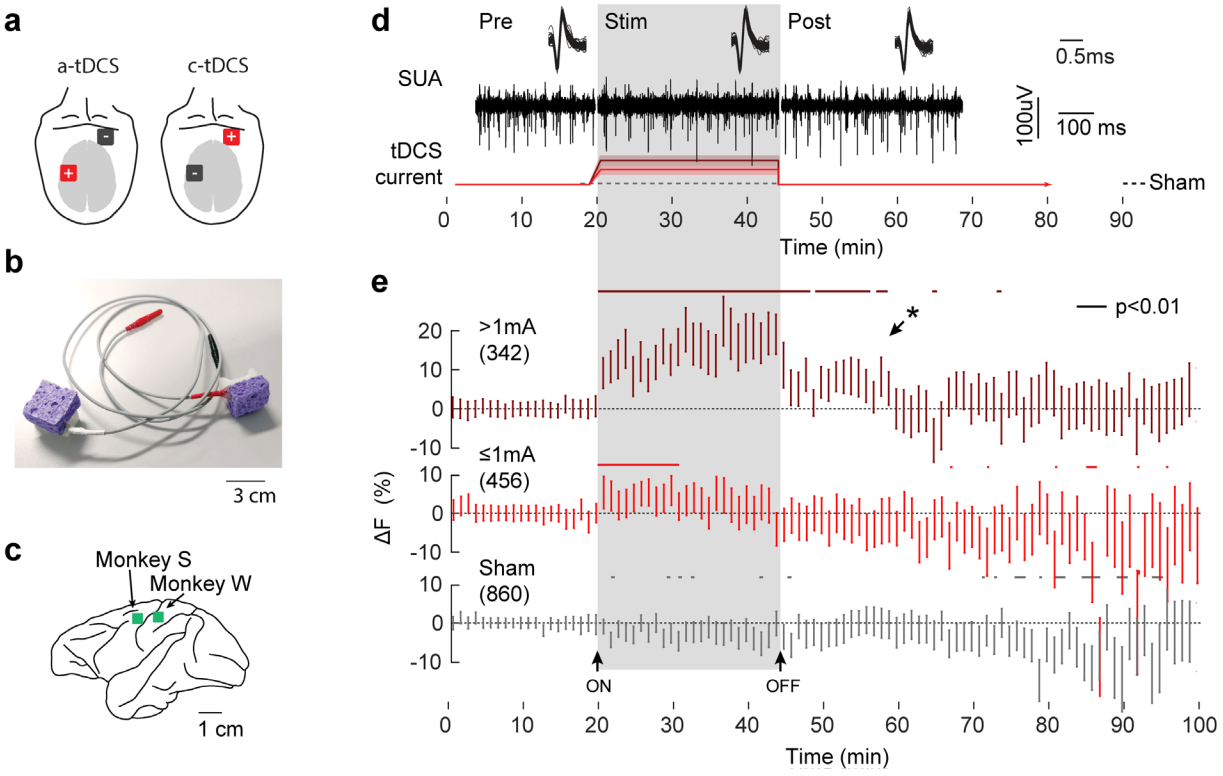

Figure 1. Simultaneous neural recording and clinical-type tDCS. **(a)** tDCS electrode montage for anodal (left) or cathodal (right) unilateral stimulation of sensorimotor cortex. **(b)** 3x3cm cellulose sponge electrodes were designed to match those used in human trials. **(c)** A microelectrode array was implanted on the gyral crown of left MI (monkey S) and left SI (Monkey W) in the areas corresponding to the right forearm. **(d)** Time-course of experiment and with example neural data. Top: sample SUA waveforms recorded during Pre, Stim (3mA a-tDCS), and Post epochs. Bottom: experiment time-line. **(e)**. Time-course of ΔF (relative to average firing in Pre) during high and low dose a-tDCS and Sham. Vertical bars: median ± 95% CI, horizontal bars: $p<0.01$, Wilcoxon sign-rank test. The Stim/Sham epoch is indicated by two arrows and light gray background.

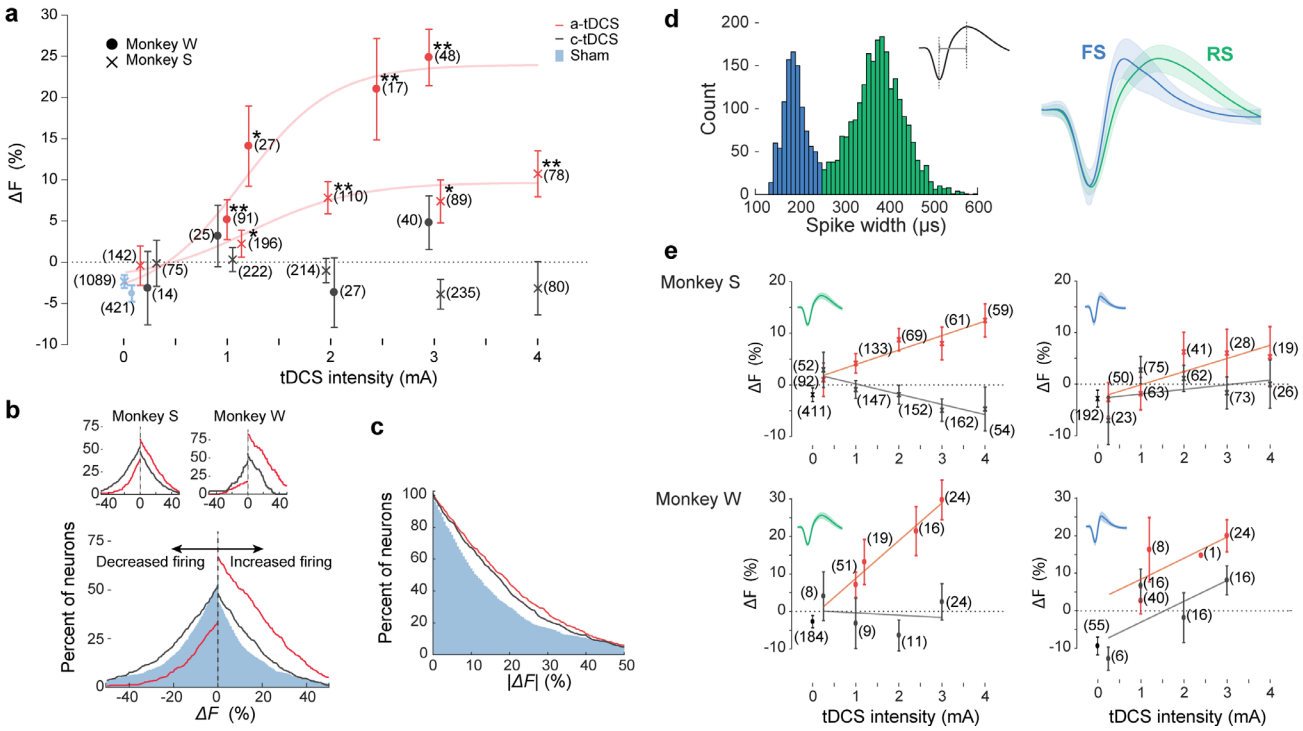

Figure 2. Firing rate changes depend on dose and cell type. **(a)** Change in firing rate (ΔF) between Pre/Stim for all recorded neurons. Average change in firing rate increased with dose during a-tDCS (red data points); the data is fitted with a sigmoidal dose-response curve *Supplementary Eq. 4* (data shows median ± 95% CI; a-tDCS: Monkey S: x_{50}=1.20mA, b=0.85 percent·mA^{-1}; Monkey W: x_{50}=1.14mA, b=1.0 percent·mA^{-1}). Effects of c-tDCS (black data points; Sham: blue data points) were masked by mixed changes in the population (two-sided Wilcoxon rank sum test tDCS vs. Sham, *p<0.01, **p<0.001 **(b)** Percent of cells with altered firing during tDCS or Sham. During a-tDCS, the percent of neurons with increased firing was greater than sham (blue area), but the percent of neurons with decreased firing dropped. During c-tDCS, the percent of neurons with altered firing (both increased or decreased rates) was higher than sham. **(c)** Percent of neurons with absolute change in firing greater than or equal to $|\Delta F|$ was similar for a- and c-tDCS. **(d-e)** Regular spiking (RS) and fast spiking (FS) neurons are differently affected by tDCS. **(d)** Histogram of spike width (trough – peak distance) for all neurons is bimodal and used to delineate two clusters (RS: ≥250μs, N=1812 and FS: <250μs, N=859). Right: average waveform of FS (blue) and RS (green) neurons (peak normalized for clarity). **(e)** Firing rates of RS cells are positivity correlated with dose during a-tDCS and negatively correlated with dose during c-tDCS (data points show median ± 95% CI. linear interpolation, $y=bx+c$. a-tDCS: Monkey S: b=2.8, R^2=0.91; Monkey W: b=10, R^2=0.96; c-tDCS: Monkey S: b=-2.0, R^2=0.87; Monkey W: b=-0.6, R^2=0.02). Firing rates of FS cells tend to increase with a- and c-tDCS. Modulation is weaker than for RS cells (a-tDCS: Monkey S: b=2.5, R^2=0.71; Monkey W: b=0.9, R^2=0.13; c-tDCS: Monkey S: b=5.6, R^2=0.52; Monkey W: b=5.5, R^2=0.48).

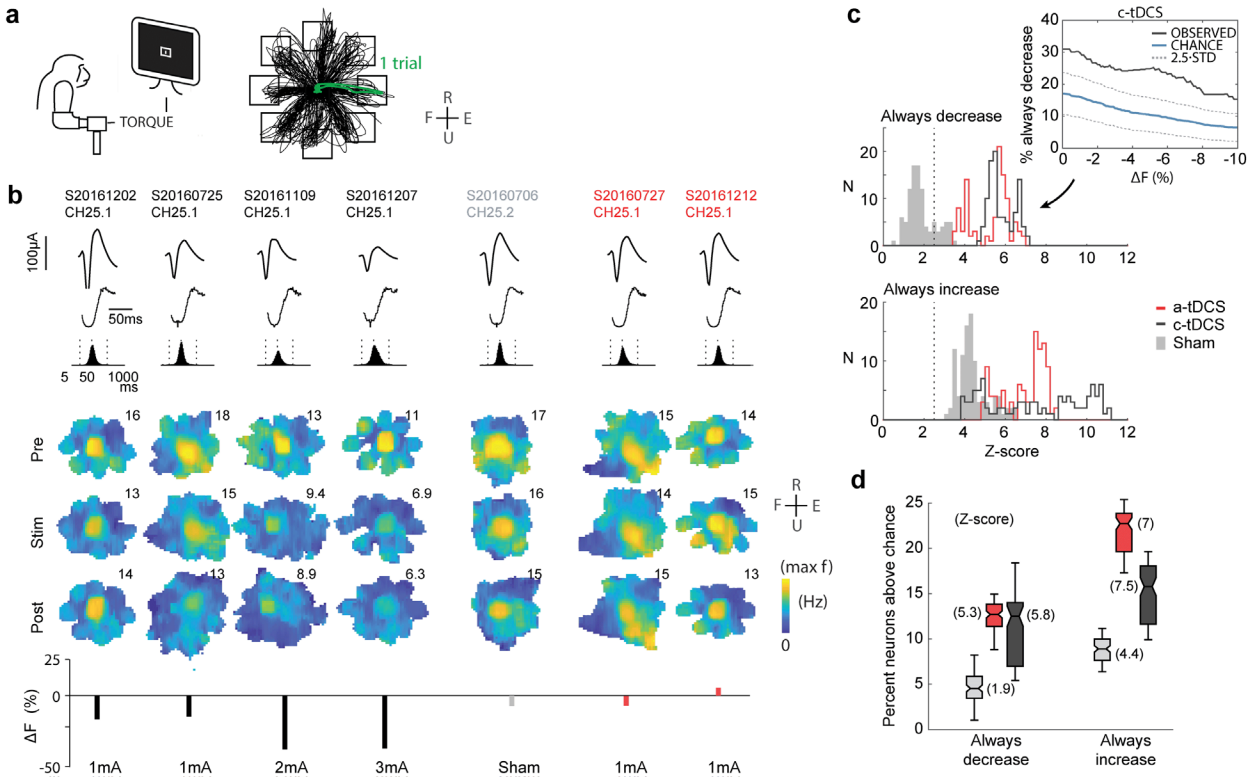

Figure 3. tDCS affects the same cells consistently across experiments. **(a)** Torque trajectories (black traces) during 10 minutes of task performance with target locations indicated by black squares. **(b)** A neuron recorded across four c-tDCS experiments **(**black**)**, 1 sham experiment **(**gray**)** and 2 a-tDCS experiments **(**red**)**. From top to bottom: average spike waveform, spike time autocorrelogram with lag [-20,100]ms (black trace), ISI distribution (black histogram), firing rate maps in torque space for Pre, Stim, and Post epochs, and percent change in spiking (bar). Cell firing rate drops with increasing c-tDCS intensity but is unaffected during sham or a-tDCS (no higher intensity a-tDCS experiments existed with this neuron). **(c)** Distribution of z-scored probability that neurons are reliably excited or inhibited by tDCS. Dashed line indicates p=0.01 relative to data shuffled within each condition (10,000 iterations). Inset: Example observed probability of consistent decreased firing during c-tDCS by at least ΔF from -10 to 0% (black trace). Chance probability ± 2.58·SD blue and dashed blue traces. **(d)** Percent of cells that always increased or decreased firing for a-tDCS, c-tDCS, or Sham experiments. Z-score relative to shuffled data indicated in parenthesis. Both a-tDCs and c-tDCS significantly increased the percent of cells that reliably increased or decreased their firing, suggesting that both polarities produce reliable, mixed effects in single neurons across sessions (z-scores>5.3, or p<0.001). Box plot center line: median, notch: 95% CI, box: upper and lower quartiles, whiskers: 1.5x interquartile range (IQR).

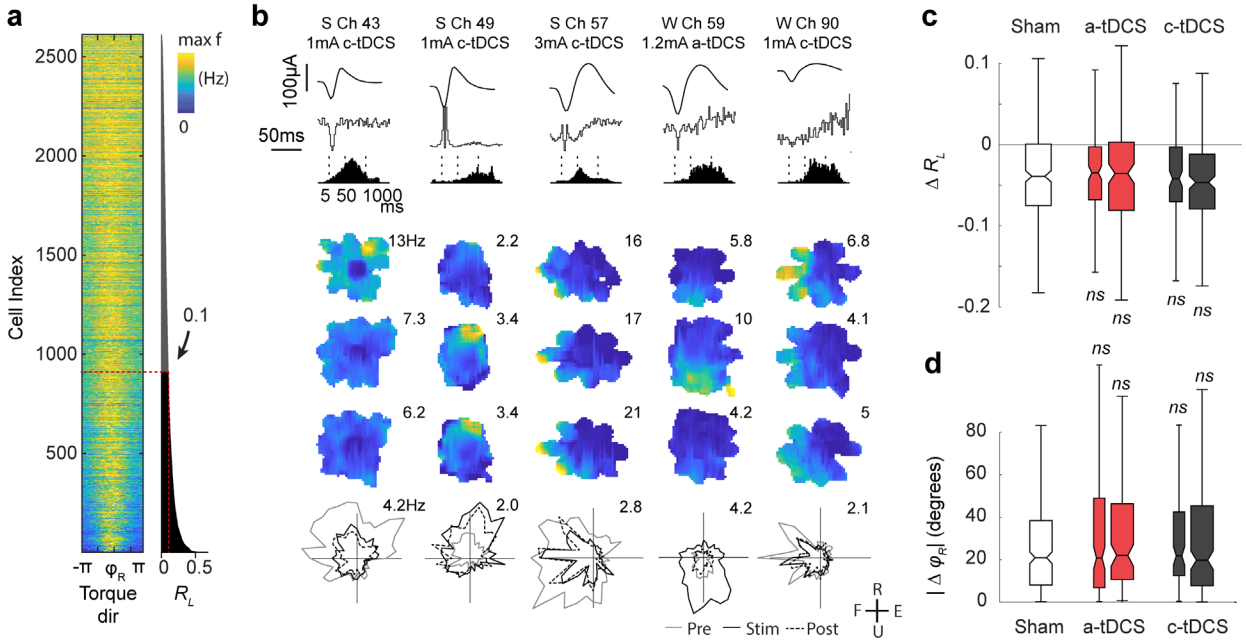

Figure 4. Directional tuning of single neurons is unaffected by tDCS. **(a)** Directional tuning functions of all neurons (peak normalized and rotated by their preferred direction) are ordered by R_L. **(b)** Five directionally tuned neurons (R_L>0.1) during a- and c-tDCS. Spiking features and rate maps as in Figure 3. While the amplitude of tuning is modulated by tDCS, directionally is preserved. **(c)** tDCS did not significantly change the strength of directional tuning as compared with Sham (low dose: thin boxes, high dose: wide boxes; p>0.05; Wilcoxon rank-sum test). There was a small but statistically significant decrease in R_L for all conditions (p<0.001; paired Wilcoxon sign-rank test). **(d)** Absolute change in preferred angle from Pre-Stim/Sham for directionally tuned neurons (R_L>0.01). tDCS did not significantly change the direction of tuning relative to sham ($|\Delta\varphi_R|$ p>0.05), and there was no bias in the population-wide changes in preferred direction for any condition ($\Delta\varphi_R$, not shown; p>0.05, Wilcoxon sign-rank test).

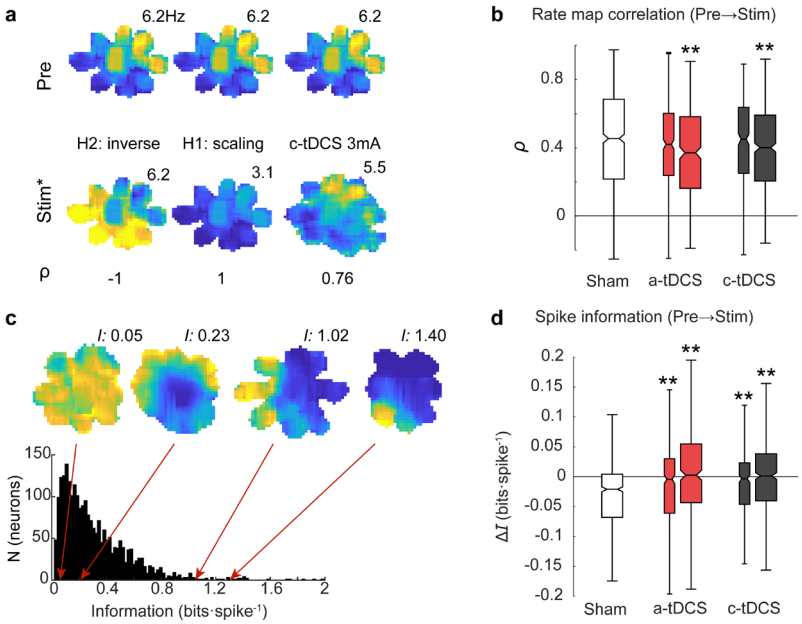

Figure 5. Small changes in torque space tuning during high dose tDCS. **(a)** Three rate map comparisons and their associated correlation coefficient (ρ) for illustrative purposes. ρ is minimal (-1) in the hypothetical case of inverted peaks/troughs, maximal (1) in the hypothetical case of single rate scaling, and high (0.76) for an example during during 3mA c-tDCS. **(b)** There were small shifts in tuning shape between Pre and Stim/Sham epochs, and this effect was more pronounced during high dose tDCS. **(c)** Histogram of all torque vector spike information content (I) for all neurons. Four example rate maps with corresponding I values above demonstrate how "peaky" neurons carry more information than do neurons with dispersed spikes. **(d)** Shifts in tuning were not associated with drops in spike information during tDCS. (**p<0.001, Wilcoxon rank-sum test). Box plot center line: median, notch: 95% CI, box: upper and lower quartiles, whiskers: 1.5x IQR.

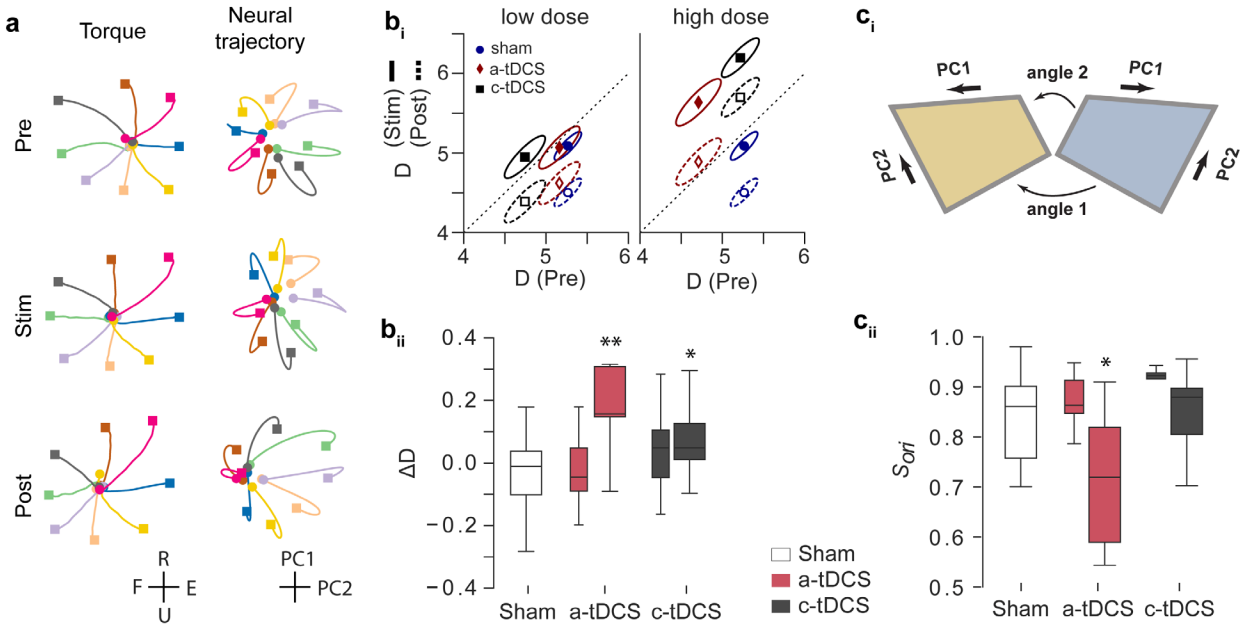

Figure 6. Population dynamics during the task and tDCS. **(a)** Target-specific, averaged manipulandum torques (left) and population firing rates projected in first two PCs (right) for an example session, not normalized for illustration (3 mA c-tDCS, N_{cells}=49). Colors indicate target identity, circle markers: t=0 seconds (target onset), square markers: t=0.5 seconds. **(b_i)** Mean dimensionality between Pre-Stim epochs (solid) and Pre-Post epochs (dashed). Points show mean of bivariate sample and ellipses show one standard error. Data points above the line (high dose tDCS during Stim and Post) indicate an increase in ensemble trajectory dimensionality, whereas points below the diagonal indicate a drop in dimensionality. Low dimensional ensemble trajectories utilize a smaller subspace of possible population patterns as compared with high dimensional trajectories. **(b_{ii})** Box plots showing statistics of Pre-normalized dimensionality change for neural trajectories during Pre and Stim. Box edges show first and third quartiles, internal bar shows mean, whiskers show extremal values. Data plotted for tDCS low (≤ 1, thin bars) and high (>1mA, thick bars) doses. **(c_i)** Illustration of principal angles between two linear PC manifolds. **(c_{ii})** Change in *orientation similarity* (S_{ori}) of manifolds (PC1 & PC2 as depicted in **a**) from Pre to Stim. S_{ori} remains high during Sham epochs, indicating that ensemble patterns are stable over time. High dose a-tDCS evoked new dominant patterns of activity in the ensemble, indicated by a decrease in S_{ori}. (*p<0.05, **p<.01, Sham vs. tDCS, independent t-test). Box plot center line: median, box: upper and lower quartiles, whiskers: 1.5x IQR.

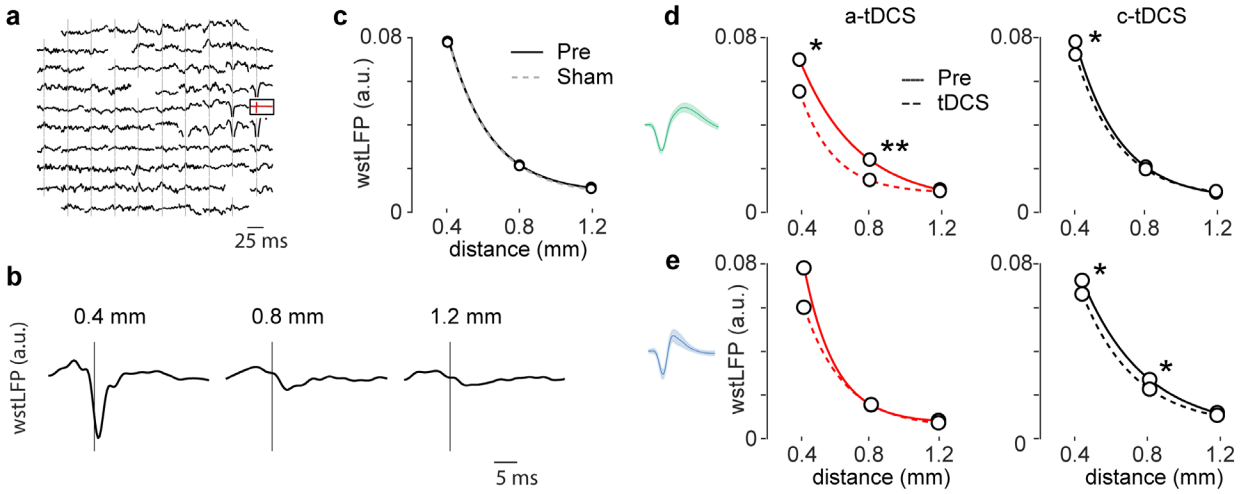

Figure 7. tDCS diminishes the amplitude of RS neuron spike-triggered LFP. **(a)** Whitened spike triggered LFP (wst-LFP) across the microelectrode array shows significant post-spike features at channels close to the neuron. **(b)** Example wst-LFP at three distances from triggering neuron (Manhattan distance). **(c)** Trough amplitude of wst-LFP (global minimum between 0 and 6ms lag) are stable from Pre to Sham epochs. The data is fitted with an exponential $A\ exp(-x/\lambda)+C$, where x is the distance and λ (0.24mm) is the space constant. **(d-e)**. Effects of high dose tDCS on RS and FS cells. (*N*, *A* and *λ* reported in *Supplemental table 1*). (**d)** Amplitude of wst-LFP at channels adjacent to RS cells is diminished by high dose a-tDCS (distance 0.4mm: $p<0.01$; 0.8mm: $p<0.001$; paired Wilcoxon sign-rank test). Effect is small, but significant for 0.4mm distance during c-tDCS ($p<0.01$). (**e)** Amplitude of wst-LFP at channels adjacent to FS cells is diminished by c-tDCS (distance 0.4mm and 0.8mm $p<0.001$) but not a-tDCS. **$p<0.001$, *$p<0.01$, paired Wilcoxon sign-rank test.

Bibliography

1. Morrell, F. Effect of anodal polarization on the firing pattern of single cortical cells. *Ann N Y Acad Sci* **92,** 860–876 (1961).

2. Bindman, L. J., Lippold, O. C. J. & Redfearn, J. W. T. Long-lasting Changes in the Level of the Electrical Activity of the Cerebral Cortex produced by Polarizing Currents. *Nature* **196,** 584–585 (1962).

3. Gartside, I. B. Mechanisms of sustained increases of firing rate of neurones in the rat cerebral cortex after polarization: role of protein synthesis. *Nature* **220,** 383–384 (1968).

4. Bindman, L. J., Lippold, O. C. & Redfearn, J. W. The Action Of Brief Polarizing Currents On The Cerebral Cortex Of The Rat (1) During Current Flow And (2) In The Production Of Long-Lasting After-Effects. *J Physiol* **172,** 369–382 (1964).

5. Creutzfeldt, O. D., Fromm, G. H. & Kapp, H. Influence of transcortical d-c currents on cortical neuronal activity. *Exp. Neurol.* **5,** 436–452 (1962).

6. Nitsche, M. A. *et al.* Pharmacological modulation of cortical excitability shifts induced by transcranial direct current stimulation in humans. *J. Physiol.* (2003). doi:10.1113/jphysiol.2003.049916

7. Stagg, C. J. *et al.* Polarity-Sensitive Modulation of Cortical Neurotransmitters by Transcranial Stimulation. *J. Neurosci.* (2009). doi:10.1523/JNEUROSCI.4432-08.2009

8. Bachtiar, V., Near, J., Johansen-Berg, H. & Stagg, C. J. Modulation of GABA and resting state functional connectivity by transcranial direct current stimulation. *Elife* (2015). doi:10.7554/eLife.08789

9. Fritsch, B. *et al.* Direct current stimulation promotes BDNF-dependent synaptic plasticity: potential implications for motor learning. *Neuron* **66,** 198–204 (2010).

10. Vöröslakos, M. *et al.* Direct effects of transcranial electric stimulation on brain circuits in rats and humans. *Nat. Commun.* **9,** (2018).

11. Lafon, B. *et al.* Low frequency transcranial electrical stimulation does not entrain sleep rhythms

measured by human intracranial recordings. *Nat. Commun.* (2017). doi:10.1038/s41467-017-01045-x

12. Nitsche, M. A. & Paulus, W. Sustained excitability elevations induced by transcranial DC motor cortex stimulation in humans. *Neurology* (2001). doi:10.1212/WNL.57.10.1899

13. Nitsche, M. A. & Paulus, W. Excitability changes induced in the human motor cortex by weak transcranial direct current stimulation. *J. Physiol.* **527,** 633–639 (2000).

14. Elsner, B., Kugler, J., Pohl, M. & Mehrholz, J. Transcranial direct current stimulation (tDCS) for improving activities of daily living, and physical and cognitive functioning, in people after stroke. *Cochrane Database of Systematic Reviews* **2016,** (2016).

15. Frank, E. *et al.* Treatment of chronic tinnitus with repeated sessions of prefrontal transcranial direct current stimulation: Outcomes from an open-label pilot study. *J. Neurol.* **259,** 327–333 (2012).

16. Fregni, F. *et al.* A sham-controlled, phase II trial of transcranial direct current stimulation for the treatment of central pain in traumatic spinal cord injury. *Pain* **122,** 197–209 (2006).

17. Kekic, M., Boysen, E., Campbell, I. C. & Schmidt, U. A systematic review of the clinical efficacy of transcranial direct current stimulation (tDCS) in psychiatric disorders. *Journal of Psychiatric Research* **74,** 70–86 (2016).

18. Marshall, L. Transcranial Direct Current Stimulation during Sleep Improves Declarative Memory. *J. Neurosci.* **24,** 9985–9992 (2004).

19. Reis, J. *et al.* Noninvasive cortical stimulation enhances motor skill acquisition over multiple days through an effect on consolidation. *Proc. Natl. Acad. Sci. U. S. A.* **106,** 1590–1595 (2009).

20. Hummel, F. C. *et al.* Effects of brain polarization on reaction times and pinch force in chronic stroke. *BMC Neurosci.* **7,** (2006).

21. Külzow, N. *et al.* No effects of non-invasive brain stimulation on multiple sessions of object-location-memory training in healthy older adults. *Front. Neurosci.* **11,** (2018).

22. Horvath, J. C., Forte, J. D. & Carter, O. Quantitative review finds no evidence of cognitive effects

in healthy populations from single-session transcranial direct current stimulation (tDCS). *Brain Stimul.* **8,** 535–550 (2015).

23. Hill, A. T., Fitzgerald, P. B. & Hoy, K. E. Effects of Anodal Transcranial Direct Current Stimulation on Working Memory: A Systematic Review and Meta-Analysis of Findings from Healthy and Neuropsychiatric Populations. *Brain Stimulation* **9,** 197–208 (2016).
24. Jamil, A. *et al.* Systematic evaluation of the impact of stimulation intensity on neuroplastic after-effects induced by transcranial direct current stimulation. *J. Physiol.* **595,** 1273–1288 (2017).
25. Batsikadze, G., Moliadze, V., Paulus, W., Kuo, M. F. & Nitsche, M. A. Partially non-linear stimulation intensity-dependent effects of direct current stimulation on motor cortex excitability in humans. *J. Physiol.* (2013). doi:10.1113/jphysiol.2012.249730
26. Ridding, M. C. & Ziemann, U. Determinants of the induction of cortical plasticity by non-invasive brain stimulation in healthy subjects. *Journal of Physiology* (2010). doi:10.1113/jphysiol.2010.190314
27. Horvath, J. C., Carter, O. & Forte, J. D. Transcranial direct current stimulation: five important issues we aren't discussing (but probably should be). *Front. Syst. Neurosci.* **8,** (2014).
28. Kar, K., Duijnhouwer, J. & Krekelberg, B. Transcranial Alternating Current Stimulation Attenuates Neuronal Adaptation. *J. Neurosci.* **37,** 2325–2335 (2017).
29. Opitz, A. *et al.* Spatiotemporal structure of intracranial electric fields induced by transcranial electric stimulation in humans and nonhuman primates. *Sci. Rep.* (2016). doi:10.1038/srep31236
30. Huang, Y. *et al.* Measurements and models of electric fields in the in vivo human brain during transcranial electric stimulation. *Elife* **6,** (2017).
31. Radman, T., Ramos, R. L., Brumberg, J. C. & Bikson, M. Role of cortical cell type and morphology in subthreshold and suprathreshold uniform electric field stimulation in vitro. *Brain Stimul.* (2009). doi:10.1016/j.brs.2009.03.007
32. Bikson, M. *et al.* Effects of uniform extracellular DC electric fields on excitability in rat hippocampal slices in vitro. *J Physiol* **557,** 175–190 (2004).

33. Francis, J. T., Gluckman, B. J. & Schiff, S. J. Sensitivity of Neurons to Weak Electric Fields. *J. Neurosci.* (2003). doi:10.1523/JNEUROSCI.23-19-07255.2003

34. Rahman, A. *et al.* Cellular effects of acute direct current stimulation: Somatic and synaptic terminal effects. *J. Physiol.* **591,** 2563–2578 (2013).

35. Rahman, A., Lafon, B., Parra, L. C. & Bikson, M. Direct current stimulation boosts synaptic gain and cooperativity in vitro. *J. Physiol.* **595,** 3535–3547 (2017).

36. Kronberg, G., Bridi, M., Abel, T., Bikson, M. & Parra, L. C. Direct Current Stimulation Modulates LTP and LTD: Activity Dependence and Dendritic Effects. *Brain Stimul.* **10,** 51–58 (2017).

37. Anastassiou, C. A., Montgomery, S. M., Barahona, M., Buzsaki, G. & Koch, C. The Effect of Spatially Inhomogeneous Extracellular Electric Fields on Neurons. *J. Neurosci.* **30,** 1925–1936 (2010).

38. Reato, D., Rahman, A., Bikson, M. & Parra, L. C. Low-Intensity Electrical Stimulation Affects Network Dynamics by Modulating Population Rate and Spike Timing. *J. Neurosci.* (2010). doi:10.1523/JNEUROSCI.2059-10.2010

39. Zaghi, S., Acar, M., Hultgren, B., Boggio, P. S. & Fregni, F. Noninvasive brain stimulation with low-intensity electrical currents: Putative mechanisms of action for direct and alternating current stimulation. *Neuroscientist* (2010). doi:10.1177/1073858409336227

40. Cramer, S. C. Repairing the human brain after stroke. II. Restorative therapies. *Ann Neurol* **63,** 549–560 (2008).

41. Brown, J. a, Lutsep, H. L., Weinand, M. & Cramer, S. C. Motor cortex stimulation for the enhancement of recovery from stroke: a prospective, multicenter safety study. *Neurosurgery* **58,** 464–73 (2006).

42. Hummel, F. *et al.* Effects of non-invasive cortical stimulation on skilled motor function in chronic stroke. *Brain* **128,** 490–499 (2005).

43. Lindenberg, R., Nachtigall, L., Meinzer, M., Sieg, M. M. & Floel, A. Differential effects of dual and unihemispheric motor cortex stimulation in older adults. *J Neurosci* **33,** 9176–9183 (2013).

44. Horvath, J. C., Forte, J. D. & Carter, O. Evidence that transcranial direct current stimulation (tDCS) generates little-to-no reliable neurophysiologic effect beyond MEP amplitude modulation in healthy human subjects: A systematic review. *Neuropsychologia* **66,** 213–236 (2015).

45. English, D. F. *et al.* Pyramidal Cell-Interneuron Circuit Architecture and Dynamics in Hippocampal Networks. *Neuron* **96,** 505–520.e7 (2017).

46. Vigneswaran, G., Kraskov, A. & Lemon, R. N. Large Identified Pyramidal Cells in Macaque Motor and Premotor Cortex Exhibit 'Thin Spikes': Implications for Cell Type Classification. *J. Neurosci.* **31,** 14235–14242 (2011).

47. Vaidya, M. *et al.* Ultra-long term stability of single units using chronically implanted multielectrode arrays. in *2014 36th Annual International Conference of the IEEE Engineering in Medicine and Biology Society, EMBC 2014* 4872–4875 (2014). doi:10.1109/EMBC.2014.6944715

48. Richardson, A. G., Borghi, T. & Bizzi, E. Activity of the same motor cortex neurons during repeated experience with perturbed movement dynamics. *J. Neurophysiol.* **107,** 3144–54 (2012).

49. Fraser, G. W. & Schwartz, A. B. Recording from the same neurons chronically in motor cortex. *J. Neurophysiol.* **22,** 11–17 (2012).

50. Carandini, M. & Ferster, D. Membrane potential and firing rate in cat primary visual cortex. *J. Neurosci.* (2000). doi:10.1098/rspb.1986.0060

51. Isaacson, J. S. & Scanziani, M. How inhibition shapes cortical activity. *Neuron* **72,** 231–243 (2011).

52. Skaggs, W. E., McNaughton, B. L. & Gothard, K. M. in *Advances in Neural Information Processing Systems 5* (eds. Hanson, S. J., Cowan, J. D. & Giles, C. L.) 1030–1037 (Morgan-Kaufmann, 1993). doi:10.1109/PROC.1977.10559

53. Fetz, E. E. Are movement parameters recognizably coded in the activity of single neurons? *Behav. Brain Sci.* **15,** 679–690 (1992).

54. Churchland, M. M. & Shenoy, K. V. Temporal Complexity and Heterogeneity of Single-Neuron Activity in Premotor and Motor Cortex. *J. Neurophysiol.* **97,** 4235–4257 (2007).

55. Shenoy, K. V., Sahani, M. & Churchland, M. M. Cortical Control of Arm Movements: A Dynamical Systems Perspective. *Annu. Rev. Neurosci.* **36,** 337–359 (2013).

56. Sadtler, P. T. *et al.* Neural constraints on learning. *Nature* **512,** 423–426 (2014).

57. Churchland, M. M. *et al.* Neural population dynamics during reaching. *Nature* **487,** 51–56 (2012).

58. Cunningham, J. P. & Yu, B. M. Dimensionality reduction for large-scale neural recordings. *Nature Neuroscience* **17,** 1500–1509 (2014).

59. Brendel, W., Romo, R. & Machens, C. K. Demixed Principal Component Analysis. *Adv. Neural Inf. Process. Syst. 24* 2654–2662 (2011).

60. Kobak, D. *et al.* Demixed principal component analysis of neural population data. *Elife* **5,** (2016).

61. Litwin-Kumar, A., Harris, K. D., Axel, R., Sompolinsky, H. & Abbott, L. F. Optimal Degrees of Synaptic Connectivity. *Neuron* **93,** 1153–1164.e7 (2017).

62. Mazzucato, L., Fontanini, A. & La Camera, G. Stimuli Reduce the Dimensionality of Cortical Activity. *Front. Syst. Neurosci.* **10,** (2016).

63. Telenczuk, B. *et al.* Local field potentials primarily reflect inhibitory neuron activity in human and monkey cortex. *Sci. Rep.* **7,** (2017).

64. Levy, R. B. & Reyes, A. D. Spatial Profile of Excitatory and Inhibitory Synaptic Connectivity in Mouse Primary Auditory Cortex. *J. Neurosci.* **32,** 5609–5619 (2012).

65. Krause, M. R. *et al.* Transcranial Direct Current Stimulation Facilitates Associative Learning and Alters Functional Connectivity in the Primate Brain. *Curr. Biol.* **27,** 3086–3096.e3 (2017).

66. Esmaeilpour, Z. *et al.* Notes on Human Trials of Transcranial Direct Current Stimulation between 1960 and 1998. *Front. Hum. Neurosci.* **11,** (2017).

67. Lippold, 0 C J, Redfearn, J. W. T., LIPPOLD, O. C. & Redfearn, J. W. T. Mental Changes Resulting from the Passage of Small Direct Currents Through the Human Brain. *Br. J. Psychiatry* **110,** 768–772 (1964).

68. Sasaki, K. & Gemba, H. Compensatory motor function of the somatosensory cortex for the motor cortex temporarily impaired by cooling in the monkey. *Exp. Brain Res.* **55,** 60–68 (1984).

69. Fetz, E. E., Finocchio, D. V, Baker, M. A. & Soso, M. J. Sensory and motor responses of precentral cortex cells during comparable passive and active joint movements. *J. Neurophysiol.* **43,** 1070–1089 (1980).

70. Soso, M. J. & Fetz, E. E. Responses of identified cells in postcentral cortex of awake monkeys during comparable active and passive joint movements. *J. Neurophysiol.* **43,** 1090–1110 (1980).

71. Golub, M. D. *et al.* Learning by neural reassociation. *Nat. Neurosci.* **21,** 607–616 (2018).

72. Ajemian, R., D'Ausilio, A., Moorman, H. & Bizzi, E. Why professional athletes need a prolonged period of warm-up and other peculiarities of human motor learning. *J. Mot. Behav.* **42,** 381–8 (2010).

73. Ajemian, R., D'Ausilio, A., Moorman, H. & Bizzi, E. A theory for how sensorimotor skills are learned and retained in noisy and nonstationary neural circuits. *Proc. Natl. Acad. Sci. U. S. A.* **110,** E5078-87 (2013).

74. Matsumura, M., Chen, D., Sawaguchi, T., Kubota, K. & Fetz, E. E. Synaptic interactions between primate precentral cortex neurons revealed by spike-triggered averaging of intracellular membrane potentials in vivo. *J. Neurosci.* **16,** 7757–7767 (1996).